Multi-scale Analysis of Discrete Contours for Unsupervised Noise Detection*

Bertrand Kerautret[1] and Jacques-Olivier Lachaud[2]

[1] LORIA, Nancy University - IUT de Saint Dié des Vosges
54506 Vandœuvre-lès-Nancy Cedex
kerautre@loria.fr
[2] LAMA, University of Savoie
73376 Le Bourget du Lac
jacques-olivier.lachaud@univ-savoie.fr

Abstract. Blurred segments [2] were introduced in discrete geometry to address possible noise along discrete contours. The noise is not really detected but is rather canceled out by thickening digital straight segments. The thickness is tuned by a user and set globally for the contour, which requires both supervision and non-adaptive contour processing. To overcome this issue, we propose an original strategy to detect locally both the amount of noise and the meaningful scales of each point of a digital contour. Based on the asymptotic properties of maximal segments, it also detects curved and flat parts of the contour. From a given maximal observation scale, the proposed approach does not require any parameter tuning and is easy to implement. We demonstrate its effectiveness on several datasets. Its potential applications are numerous, ranging from geometric estimators to contour reconstruction.

Keywords: Noise detection, discrete contour, maximal segments.

1 Introduction

Discrete or digital contours are natural outputs of image segmentation algorithms or digitisation processes like document scanning. Being constituted of horizontal and vertical steps, they are in essence non smooth. However their geometric analysis is of primary importance for later processing such as quantitative analysis, shape recognition or shape matching. Discrete geometry provides techniques to estimate correctly geometric characteristics on such contours, when the digital contour reflects perfect data. The most accurate techniques rely generally on the extraction of *maximal segments*, which are local affine reconstruction of contours.

In most cases, digital contours are not perfect digitizations of ideal shapes but present noise and perturbations. Rather recently, *blurred segments* were introduced to take into account both the discreteness and possible noise of data

* This work was partially funded by ANR GeoDIB project, n° ANR-06-BLAN-0225. Bertrand Kerautret was partially funded by a BQR project of Nancy-Universités.

P. Wiederhold and R.P. Barneva (Eds.): IWCIA 2009, LNCS 5852, pp. 187–200, 2009.

[2]. They are parameterized with a positive value related to the thickness of the perturbation. Based on this, discrete tangent and curvature estimators robust to noise have been developed [10,5]. Similarly, the curvature estimator of [9] requires a smoothing parameter related to the amount of noise.

Two factors limit the applicability of these techniques: first their parameterization requires a user supervision, secondly this parameter is global to the shape, while the amount of noise may be variable along the shape. This problem has been studied a lot in the image processing and edge detection community and led to the development of multi-scale analysis [11,6]. Further improvements lead to the automatic determination of a local scale [4,1]. This scale gives the minimum amount of local smoothing necessary to capture the local image geometry (i.e. edges). These techniques are thus able to determine the local amount of noise: adaptive filtering is then possible (generally edge detection).

Although very interesting for image processing, they cannot be used to process binary images or, equivalently, digital contours. They indeed rely on a local SNR analysis of the image, sometimes with a user-given global SNR parameter. Since we have only the discrete contour as input, the SNR is not calculable. We propose here a new method for estimating locally if the digital contour is damaged, what is the amount of perturbation, and what are the meaningful scales at which this part of the contour should be considered. Our method is similar in spirit to multi-scale analysis, but relies on specific properties of digital contours. The main idea is to look for the asymptotic properties of maximal segments in the multiresolution decomposition of the given contour. If they are present, then the scale is meaningful, otherwise the contour is still noisy at this scale and must be examined at a coarser scale. Our approach is local, requires no parameter tuning (from a given maximal observation scale), and is easy to implement. Its output can be used in many applications which requires a global or local noise parameterization. Among them, we may quote tangent or curvature estimators, dominant point and corner detection.

In Section 2 we recall standard notions of discrete geometry and known asymptotic results on maximal segments. We show that the length of maximal segments over scales can be used both to distinguish between flat and curved parts of a contour and to detect noise. In Section 3 we validate our technique on several datasets, containing different shape geometries, localized and variable noise, various resolutions. All datasets are processed without any specific parameterization. Noise is correctly determined in all cases. Section 4 presents some perspectives to this work.

2 Scale Properties of Maximal Segments

2.1 Definition and Known Asymptotic Results

A *standard digital straight line (DSL)* is some set $\{(x, y) \in \mathbb{Z}^2, \mu \leq ax - by < \mu + |a| + |b|\}$, where (a, b, μ) are also integers and $\gcd(a, b) = 1$. It is well known that a DSL is a 4-connected simple path in the digital plane. A *digital straight segment (DSS)* is a 4-connected piece of DSL. The interpixel contour of a simple

digital shape is a 4-connected closed path without self-intersections. Given such a 4-connected path C, a *maximal segment* M is a subset of C that is a DSS and which is no more a DSS when adding any other point of $C \setminus M$.

We recall some asymptotic results related to maximal segments that lie on the boundary of some shape X digitized with step h. The digitization process is $\mathrm{Dig}_h(X) = X \cap h\mathbb{Z} \times h\mathbb{Z}$ (Gauss digitization). First, we assume the shape has smooth C^3-boundary and is strictly convex (no flat zones, no inflexion point). Theorem 5.26 of [7] states that the smallest discrete length of the maximal segments on the boundary of $\mathrm{Dig}_h(X)$ is some $\Omega(1/h^{1/3})$. The longest discrete length of the maximal segments on the boundary of $\mathrm{Dig}_h(X)$ is some $O(1/h^{1/2})$ (Lemma 15 of [8]).

Secondly, we observe maximal segments along the digitization of a flat zone of a shape. Since digital straight segments are digitization of straight line segments, there is at least one maximal segment that covers the straight line. It means that the discrete length of the longest maximal segment is some $\Theta(1/h)$.

As a corollary to the previous properties, we obtain:

Corollary 1. *Let S be a simply connected shape in R^2 with a piecewise C^3 boundary. Let p be a point of the boundary ∂S of S. Consider now an open connected neighborhood U of p on ∂S. Let (L_j^h) be the digital lengths of the maximal segments along the boundary of* $\mathrm{Dig}_h(S)$ *and which cover p. Then*

$$\text{if } U \text{ is strictly convex or concave, then } \Omega(1/h^{1/3}) \leq L_j^h \leq O(1/h^{1/2}) \quad (1)$$

$$\text{if } U \text{ has null curvature everywhere, then } \Omega(1/h) \leq L_j^h \leq O(1/h) \quad (2)$$

The first inequality expresses the asymptotic behaviour of the length of maximal segments in smooth curved parts of a shape boundary. The second one gives the analog properties in flat parts of a shape boundary.

2.2 From Asymptotic to Scale Analysis by Subsampling

In the context of image analysis and pattern recognition, we do not have access to asymptotic digitizations of shapes: we are not able to get finer and finer versions of the object. At first glance, it could mean that asymptotic properties are not useful to analyze shape boundaries. This is not true. We can use asymptotic properties in a reverse manner. We consider that our digital object O is the digitization of some Euclidean shape X at a grid step h, choosing for instance again the Gauss digitization. We then subsample the digital object O with covering "pixels" of increasing sizes $i \times i$, for $i = 2, 3, \ldots, n$. The subsampling process ϕ_i will be detailed in Section 2.3. The family of digital objects $\phi_n(O), \ldots, \phi_2(O), O$ is an approximation of the finer and finer digitized versions of X, $\mathrm{Dig}_{nh}(X), \ldots, \mathrm{Dig}_{2h}(X), \mathrm{Dig}_h(X)$. Corollary 1 holds for the latter family. Although this corollary does not formally hold for the former family, a similar behaviour is observed in practice.

When looking at lengths of maximal segments around some point P of the boundary of O, we should thus observe a decreasing sequence of lengths for the

increasing sequence of digitization grid steps $h_i = ih$, whose slope is related to the fact that P was in a flat or curved region. More precisely, letting $(L_j^{h_i})_{j=1..l_i}$ be the discrete lengths of the maximal segments along the boundary of $\phi_i(O)$ and covering P, we can expect:

- If P is in a curved convex or concave zone, then the lengths $L_j^{h_i}$ follow (1).
- If P is in a flat zone, then the lengths $L_j^{h_i}$ follow (2).

The asymptotic bounds of these equations suggest:

Property 1 (Multi-scale). The plots of the lengths $L_j^{h_i}$ in log-scale should be approximately affine with negative slopes as specified below:

plot	expected slope (curved part)	(flat part)
$(\log(i), \log(\max_{j=1\ldots l_i} L_j^{h_i}))$	$\approx -\frac{1}{2}$	≈ -1
$(\log(i), \log(\min_{j=1\ldots l_i} L_j^{h_i}))$	$\approx -\frac{1}{3}$	≈ -1

The plot is only approximately affine since the preceding properties are asymptotic. Given an object at a finite resolution, subsampling induces length variations that follow only approximately the asymptotic behaviour. Arithmetic artefacts play also a role in this. It is however clear that the approximation gets better when the initial shape is digitized with a finer resolution.

We can make several remarks about the preceding result. First, it allows to distinguish between flat parts and curved parts of an object boundary, provided the object was digitized with a reasonable precision. This distinction relies only on the classification of the plot slope between $[-1, -\frac{1}{2}[$ and $[-\frac{1}{2}, -\frac{1}{3}]$. Secondly, the preceding approach is not valid on (around) points that are (i) a transition between a flat and a curved part, (ii) corner points. Thirdly, this technique assumes smooth objects with perfect digitization: if the digital contour has been damaged by noise or digitization artefacts, these characterizations do not hold.

Although the two last remarks seem problematic for analyzing shapes, we will use them to detect *locally* the amount of noise and to extract *local* meaningful scales.

2.3 Subsampling of a Digital Contour

Our multi-scale analysis of digital contours will require several subsampling computation of the initial digital shape. A common way for subsampling a binary image by integer factors $i \times i$ is to cover the pixel space with a tiling of squares of size $i \times i$. Any big pixel of the subsampled object is lighted whenever any of the covered pixel are lighted. More formally,

$$\phi_i^{x_0,y_0}(O) = \left\{(X,Y) \in \mathbb{Z}^2 | \exists (x,y) \in O, X = (x - x_0) \div i, Y = (y - y_0) \div i\right\}, \tag{3}$$

where (x_0, y_0) defines the origin of the big pixels in $\mathbb{Z}^2$ and the integer division $\div$ is defined by truncation.

Also effective, this technique has two drawbacks. First, it does not give directly a correspondence between the digital contour of O and the digital contour of the subsampling of O (such a correspondence is illustrated in Fig. 1 (b)). We need it for computing the maximal segments at a lower resolution and assigning their lengths to the desired point. Secondly, the topology of O may change through the subsampling, for instance from a simply connected shape to a shape with holes or vice versa. A point P on the contour of O may have no point in the subsampling that is in its vicinity.

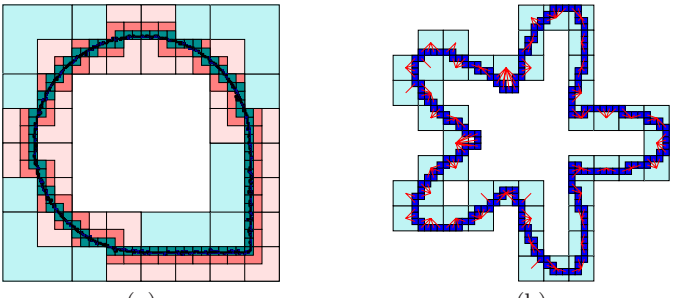

(a) (b)

Fig. 1. (a) Subsampling $\phi_i^{0,0}(C)$ of a digital contour for $i = 64, 32, 16$ and 8. (b) The function $f_4^{0,0}$ is drawn with lines joining each pixel of C to it associated pixel of $\phi_4^{0,0}(C)$.

Although the preceding problems could be solved by *ad hoc* rules, we take another road. The subsampling is not spatial but operates on the digital contour. Its output is also a digital contour. We proceed in four steps, given a digital 4-connected contour C that is the boundary of the set of pixels O in the cellular model:

1. The interpixel contour C is shifted toward the inside so that it defines the 4-connected inner border of O. This 4-connected contour of pixels is denoted by C'. It is not necessarily simple and may contain some back-and-forth paths that are oriented toward the exterior of O (*outer spikes*).
2. The pixel contour C' is subsampled as the pixel contour C'', composed of the sequence of points $(X_j, Y_j) = ((x_j - x_0) \div i, (y_j - y_0) \div i)$, where C' is the sequence of points (x_j, y_j).
3. Consecutive identical pixels of C'' are merged to get a pixel contour C'''.
4. Outer and inner spikes of C''' are removed (by several linear scans). The obtained contour is shifted toward the outside so that it defines a 4-connected interpixel contour, that is the boundary of some digital shape.

The output subsampled contour is denoted by $\phi_i^{x_0,y_0}(C)$. Note that in the four preceding steps we keep the index correspondence between the contours. Along with $\phi_i^{x_0,y_0}$, there is thus a surjective map $f_i^{x_0,y_0}$ which associates any point P in

C to its image point in the subsampled contour $\phi_i^{x_0,y_0}(C)$. Several subsampled contours are illustrated on Fig. 1 (a) and a map $f_4^{0,0}$ for another contour is shown in (b). It is worth to note that this subsampling, similar to the common spatial one, can be done either locally around the point of interest or globally for the whole contour.

2.4 Local Geometric Evaluation with Multi-scale Criterion

We are now in position to analyze the local geometry of some point P on a digital contour C. For a resolution i and a shift (x_0, y_0), we compute the discrete lengths $L_j^{h_i,x_0,y_0}$ of the maximal segments of $\phi_i^{x_0,y_0}(C)$ containing $f_i^{x_0,y_0}(P)$. To take into account the possible digitization artefacts and approximations, we average these lengths as $\overline{L}^{h_i} = \frac{1}{i^2} \sum_{0 \leq x_0 < i, 0 \leq y_0 < i} \frac{1}{l_i^{x_0,y_0}} \sum_j L_j^{h_i,x_0,y_0}$, where $l_i^{x_0,y_0}$ represents the number of maximal segments containing $f_i^{x_0,y_0}(P)$. Note that all the maximal segments of $\phi_i^{x_0,y_0}$ can be computed in linear time with the number of points [8]. Fig. 2 illustrates the maximal segments obtained on the subsampled contour with several shift values.

The *multi-scale profile* $\mathcal{P}_n(P)$ of a point P on the boundary of a digital object O is the sequence of samples $(\log(i), \log(\overline{L}^{h_i})_{i=1..n}$. According to Property 1, these samples should be correctly approached with an affine model. We thus define the *ideal multi-scale criterion* $\mu_n(P)$ of a point P on the boundary of a digital object O as the slope coefficient of the simple linear regression of $\mathcal{P}_n(P)$ (in the order regressor, regressand).

Property 1 indicates that $\mu_n(P)$ should be around -1 if P is in a flat zone, whereas it should be within $[-1/2, -1/3]$ if P is in a strictly convex or concave zone. Theorem 5.1 of [3] indicates that it is more likely to be around $-1/3$ in the latter case.

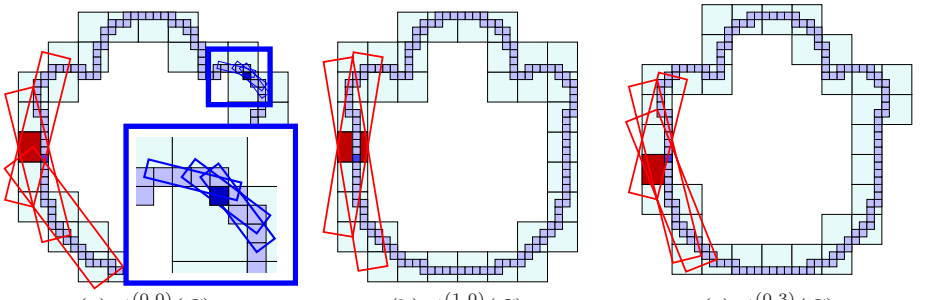

(a) $\phi_4^{(0,0)}(C)$ (b) $\phi_4^{(1,0)}(C)$ (c) $\phi_4^{(0,3)}(C)$

Fig. 2. Illustration of the maximal segments covering a point of the initial contour C (closeup view (a)). Several subsampled contours $\phi_4^{(x_0,y_0)}(C)$ obtained with different shifts with resolution 4 are given in light color (a-c). For each shift the maximal segments covering the considered point are drawn in dark.

Table 1. Distribution of the slopes of the multi-scale lengths of maximal segments (when plotted in log-space) for two different kinds of shapes generated with several digitization steps h. Two top groups: distribution for shapes with strictly positive curvature. Two bottom groups: distribution for shapes composed of flat sides. The last row gives the best choice of threshold $t_{f/c}$ to decide between flatness and curvedness for two shapes, assuming normal distribution. E and σ represent respectively the mean and the standard deviation of the slope distribution.

		distribution of slopes $\mu_n(\cdot)$ according to digitization step h				
shape X	intervals	$h = 1$	$h = 1/2$	$h = 1/4$	$h = 1/8$	$h = 1/16$
circle $r = 20$	$\in]-\infty, -\frac{2}{3}[$	0 %	0 %	0 %	0 %	0 %
	$\in [-\frac{2}{3}, -\frac{1}{2}[$	0 %	0 %	0 %	0 %	0 %
	$\in [-\frac{1}{2}, -\frac{1}{3}]$	100 %	54.0 %	62.1 %	67.0 %	58.5 %
	$\in]-\frac{1}{3}, -\frac{1}{6}]$	0 %	46.0 %	37.9 %	33.0 %	41.5 %
	$\in]-\frac{1}{6}, +\infty[$	0 %	0 %	0 %	0 %	0 %
	E, σ	$-0.391, 0.028$	$-0.359, 0.046$	$-0.356, 0.041$	$-0.343, 0.035$	$-0.342, 0.055$
ellipse $a = 20$ $b = 14$ $\theta = 0.2$	$\in]-\infty, -\frac{2}{3}[$	0 %	0 %	0 %	0 %	0 %
	$\in [-\frac{2}{3}, -\frac{1}{2}[$	5.9 %	0 %	4.4 %	2.4 %	0 %
	$\in [-\frac{1}{2}, -\frac{1}{3}]$	91.2 %	95.6 %	73.3 %	56.6 %	57.7 %
	$\in]-\frac{1}{3}, -\frac{1}{6}]$	2.9 %	4.4 %	22.3 %	41.0 %	42.3 %
	$\in]-\frac{1}{6}, +\infty[$	0 %	0 %	0 %	0 %	0 %
	E, σ	$-0.412, 0.047$	$-0.392, 0.039$	$-0.377, 0.054$	$-0.353, 0.056$	$-0.346, 0.056$
triangle $r = 20$ $\theta = 0.3$	$\in]-\infty, -\frac{5}{4}[$	0 %	0 %	0 %	0 %	0 %
	$\in [-\frac{5}{4}, -1[$	0 %	6.4 %	15.8 %	12.3 %	7.5 %
	$\in [-1, -\frac{3}{4}[$	81.2 %	89.8 %	83.8 %	87.6 %	92.4 %
	$\in [-\frac{3}{4}, -\frac{1}{2}[$	18.8 %	3.8 %	0.4 %	0.1 %	0.1 %
	$\in [-\frac{1}{2}, +\infty]$	0 %	0 %	0 %	0 %	0 %
	E, σ	$-0.860, 0.100$	$-0.931, 0.060$	$-0.956, 0.052$	$-0.923, 0.068$	$-0.920, 0.047$
pentagon $r = 20$ $\theta = 0.2$	$\in]-\infty, -\frac{5}{4}[$	0 %	0 %	0 %	0 %	0 %
	$\in [-\frac{5}{4}, -1[$	0 %	0 %	0.7 %	5.7 %	9.0 %
	$\in [-1, -\frac{3}{4}[$	37.3 %	89.3 %	95.8 %	91.2 %	89.6 %
	$\in [-\frac{3}{4}, -\frac{1}{2}[$	60.7 %	10.6 %	3.5 %	3.1 %	1.4 %
	$\in [-\frac{1}{2}, +\infty]$	2.0 %	0 %	0 %	0 %	0 %
	E, σ	$-0.695, 0.081$	$-0.815, 0.070$	$-0.890, 0.064$	$-0.914, 0.066$	$-0.924, 0.059$
$t_{f/c}$ ellipse/pentagon		-0.52	-0.55	-0.61	-0.61	-0.63

We have checked Property 1 on digitization of various smooth or polygonal shapes at different scales (from digitization step $h = 1$ to $1/16$). For each experiment, we have chosen $n = 10$. The results are summed up in Table 1. They clearly back up our claim on the validity of Property 1 as a reverse analog to asymptotic properties.

The preceding experiments suggest a flat/curved threshold $t_{f/c}$ between -0.6 and -0.5. Since the resolution of objects is generally low, setting $t_{f/c} = -0.52$ is a reasonable choice. It induces more than 98.3% of correct decision at $h = 1$, and more than 99.9% of correct decision at finer grid steps.

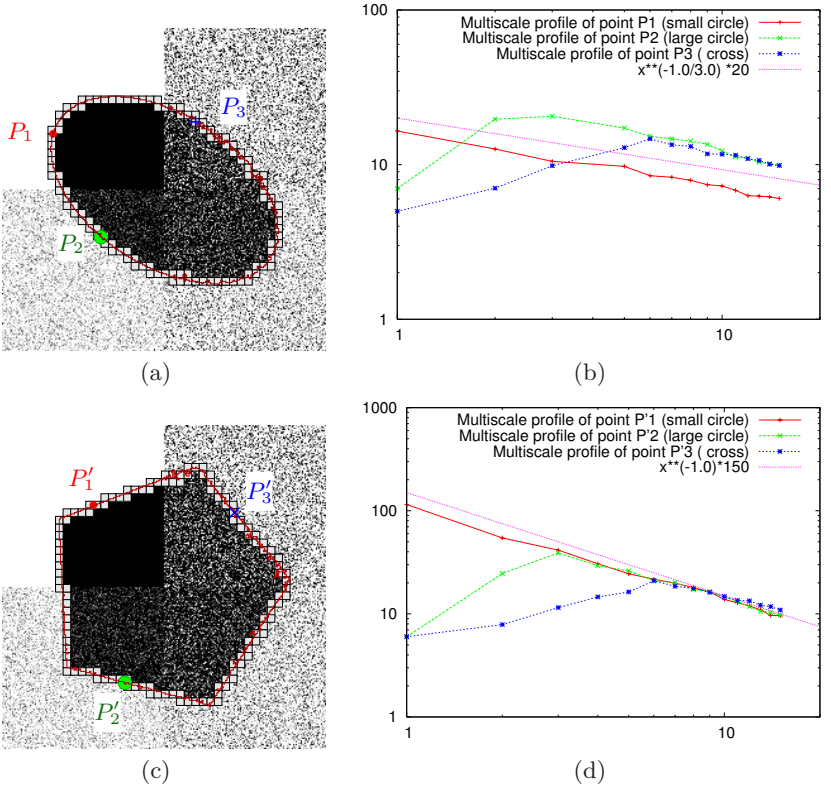

Fig. 3. Examples of multiscale profiles $\mathcal{P}_{15}(P)$ on ellipse (a,b): P_1 in a curved zone, P_2 in a slightly perturbated curved zone , P_3 in a strongly perturbated curved zone. Gaussian noise was added on each areas containing the point P_1, P_2 and P_3 with respectively the following standard deviation $\sigma_1 = 0$, $\sigma_2 = 75$, and $\sigma_2 = 175$. The same experimentation is applied on the polygon (c-d) with the points P'_1, P'_2, and P'_3.

2.5 Detecting Noise and Local Meaningful Scale

The multi-scale profile can be used to detect noisy digital contours. Indeed, if the multi-scale profile of some point P is not some approximation of an affine map with negative slope, it means that locally around P the shape geometry is neither a flat or curved zone. We display on Fig. 3 (a-b) the multi-scale profile of a point P_1 located on a perfectly digitized curved zone and the multi-scale profiles of the points P_2 and P_3 located in noisy zones. On the former profile, the decreasing affine relation is immediately visible. On the latter profiles, it is somewhat randomly increasing for fine resolution and then follow an expected decreasing affine profile after a given scale. A similar behaviour is observable for the multi-scale profiles on the pentagon shape with similar noisy regions. The only difference is the slope of the affine relation of the profiles (slopes near $-\frac{1}{3}$ for the plots of Fig. 3 (b) and near -1 for the plots of Fig. 3 (d)).

We therefore introduce a *noise threshold* t_m which discriminates between a curved zone and a noisy zone. This threshold should be somewhere between $]-\frac{1}{3},0[$. According to Table 1, setting $t_m = -1/6 \approx E + 3\sigma$ induces more than 99.7% of correct determination with some hypotheses (especially normal distribution). However after several experiments on noisy shapes it appears that the use of the upper threshold value $t_m = 0$ gives better results especially in curved zones.

A *meaningful scale* of a multi-scale profile $(X_i, Y_i)_{1 \leq i \leq n}$ is then a pair (i_1, i_2), $1 \leq i_1 < i_2 \leq n$, such that for all i, $i_1 \leq i < i_2$, $\frac{Y_{i+1}-Y_i}{X_{i+1}-X_i} \leq t_m$, and the preceding property is not true for $i_1 - 1$ and i_2.

If (i_1, i_2) is a meaningful scale of the profile $\mathcal{P}_n(P)$, the (i_1, i_2)-*multi-scale criterion* $\mu_{i_1,i_2}(P)$ of point P is then the slope coefficient of the simple linear regression of $\mathcal{P}_n(P)$ restricted to its samples from i_1 to i_2.

Obviously meaningful scales of $\mathcal{P}_n(P)$ do not overlap and are thus naturally ordered. If the first meaningful scale of $\mathcal{P}_n(P)$ is (k_1, k_2), then the integer $k_1 - 1$ is called the *noise level* at point P and we denote it by $\nu(P)$.

We will show in the experiment section that both definitions of meaningful scales and noise level have a clear intuitive interpretation. They determine precisely where the contour is perturbated and how it should be interpreted to be meaningful.

3 Experiments

Noise Detection. A robust noise detector should not detect noise on perfectly digitized data and should not be sensitive to the object initial resolution. To experiment this properties, different shapes have been generated with a manual addition of noise on some specifics areas (Fig. 4). These noisy areas are highlighted by red boxes on subfigures (a-c) and (g-i). Note that for certain areas (on bottom left on the shape) only one or three pixels were changed (highlighted in red). For each pixel P of the initial contour, the result of the noise detection is illustrated by drawing its associated pixel $f_K^{0,0}(P)$ (of size K) where K is $\nu(P) + 1$, i.e. its first meaningful scale.

The obtained noise detection displayed on Fig. 4 (d-f,j-l) shows a good precision. Even with low resolution shapes and with a one pixel change, the noise is well detected. Only a few false positive noise detections can be seen on some small areas on the flower (near corners): however these errors are limited to one noise level. Note that for all of these experiments no parameter was changed for the detection. The variable t_m associated to the noise threshold was set to 0 for all the experiments as suggested in section 2.5. The maximal resolution n used in the definition of the *multi-scale profile* $\mathcal{P}_n(P)$ has only an influence on the level of scale of the detected noise. Indeed, for example the use of the minimal value of $n = 2$ induces a noise detection only at scales 1 and 2. This value was set to 15 in all the presented experiments.

After experimenting the noise detection on shapes containing some local noisy parts, we apply this detection on a shape globally damaged with different noise

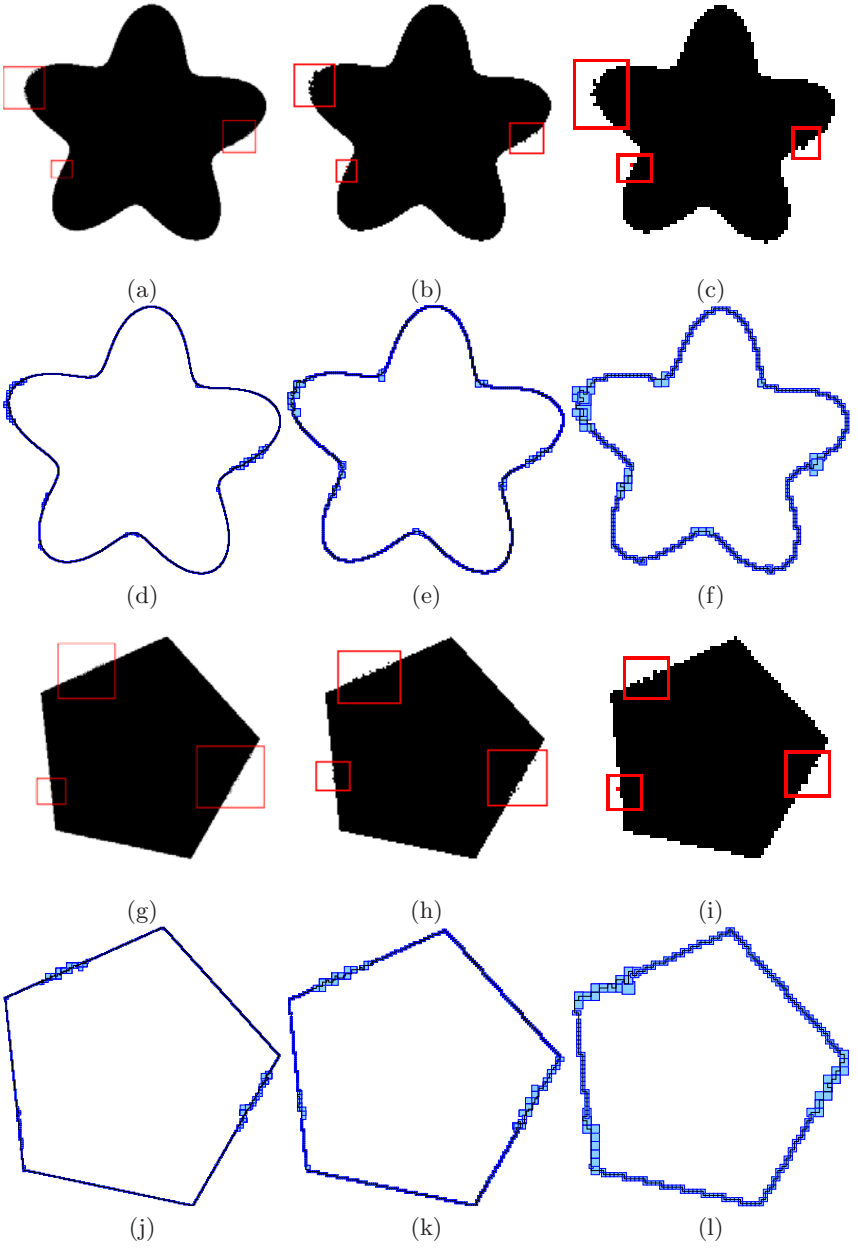

Fig. 4. Noise detection on flower-like and polygonal shapes defined with several grid sizes. Noisy areas are highlighted by red box (images (a-c,g-i)). Images (d-f,j-l) display for each pixel P its associated pixel $f_K^{0,0}(P)$ with K equal to $\nu(P)+1$.

intensities. The initial image of the shape is thus divided into 4 parts on which a gaussian noise is applied with four standard deviations $\sigma_0 = 0$, $\sigma_1 = 75$, $\sigma_2 = 125$ and $\sigma_3 = 175$. The discrete contour is then extracted from the set of the biggest connected component selected with the threshold value 128 (Fig. 5). Subimages (a-d) shows the points whose noise level is below some scale K. We can see that the original local repartition of the noise per image quadrant is well visible.

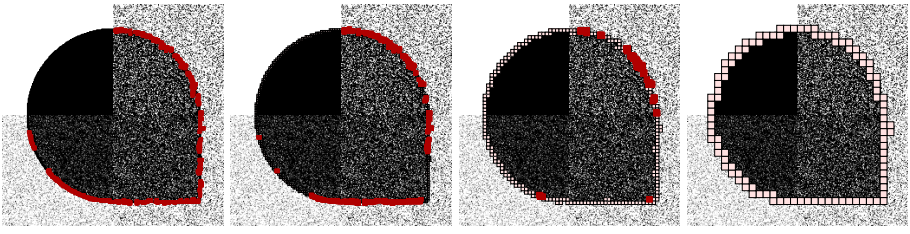

(a) $K = 1$ (b) $K = 2$ (c) $K = 4$ (d) $K = 8$

Fig. 5. Illustration of the contour parts which are considered as valid on the scale less or equals to K (light grey). Pixels with a higher noise level are drawn in dark red.

Detection of Flat and Curved Contour Areas. As described in the previous section the analysis of the *multi-scale profile* $\mathcal{P}_n(P)$ can discriminate the curved and flat areas of the contour. This discrimination relies on a constant threshold value $t_{f/c}$ which is set to -0.52 to maximize the good detection as suggested in Section 2.4. Exactly as in previous experimentations, the maximal resolution n of the *multi-scale profiles* was not changed (set to 15) and has only a limited influence since the estimation of the slope is only done within meaningful scales.

In the same way than as the noise detection, a shape containing curved and flat areas was generated with several resolutions and with gaussian noise (see Fig. 6 (a-c)). For the noisy version of the shapes, the profile analysis was initiated from the scale 4. This value was deduced from the global level of noise of the image. We can see on these examples that the curved and flat areas are well detected (subimages (a,b)) and the noisy shape (subimage (c)) presents very few pixels incorrectly classified. Fig. 6 (d-g) shows also other good detections.

Experiments on Real Images. Our method was applied on two real images with unchanged parameters (Fig. 7 and Fig. 8). The contours were obtained by extraction of the connected components defined with a simple threshold value. The image of Fig. 8 (a) was directly extracted without subsampling from a digital camera picture obtained at resolution 4000×2672 with a sensibility of 250 ISO. As for the previous experiments, the detected noise level K is illustrated by drawing for each pixel P its associated pixel $f_K^{0,0}(P)$ (Fig. 7 (a)). For the contours of Fig. 8 we change the noise visualisation by using a box of size K centered on each point. These results are comparable to the ones obtained on synthetic images and even for the detection of flat areas which are well detected (Fig. 7 (b)).

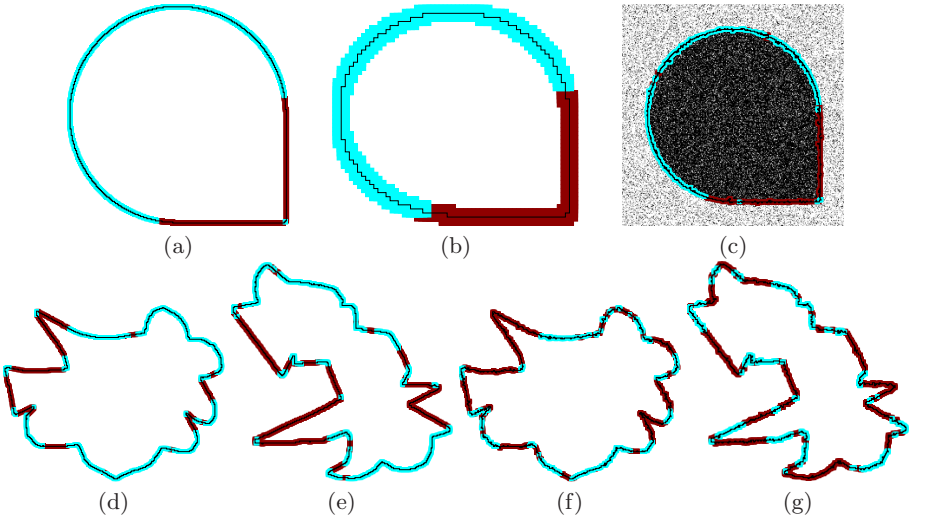

Fig. 6. Detection of flat/curved areas on a fine (a) and coarse (b) grid size, and with Gaussian noise with standard deviation 100 (c). Images (f,g) are the noisy version of (d,e) obtained after adding noise . For the shapes (c,f,g) the scale analysis was initiated from the scale 4.

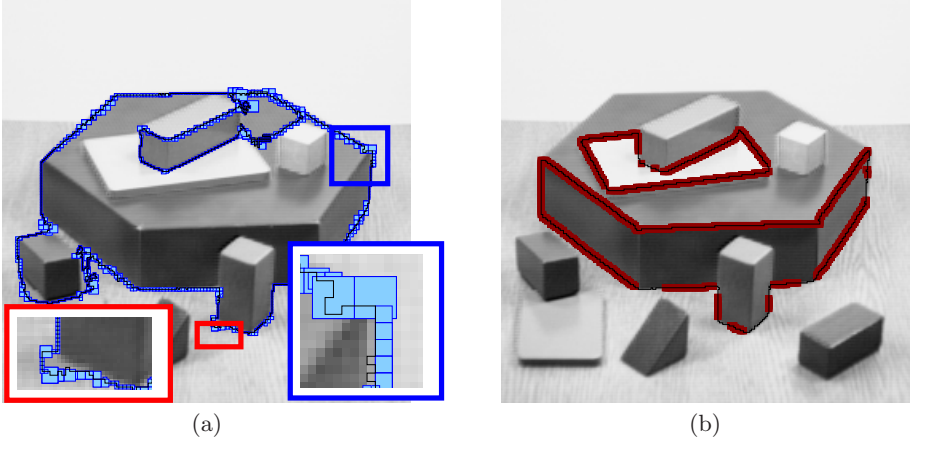

Fig. 7. (a) Example of meaningful scales obtained on contours in a real image (a). (b) Detection of the flat areas of selected contours.

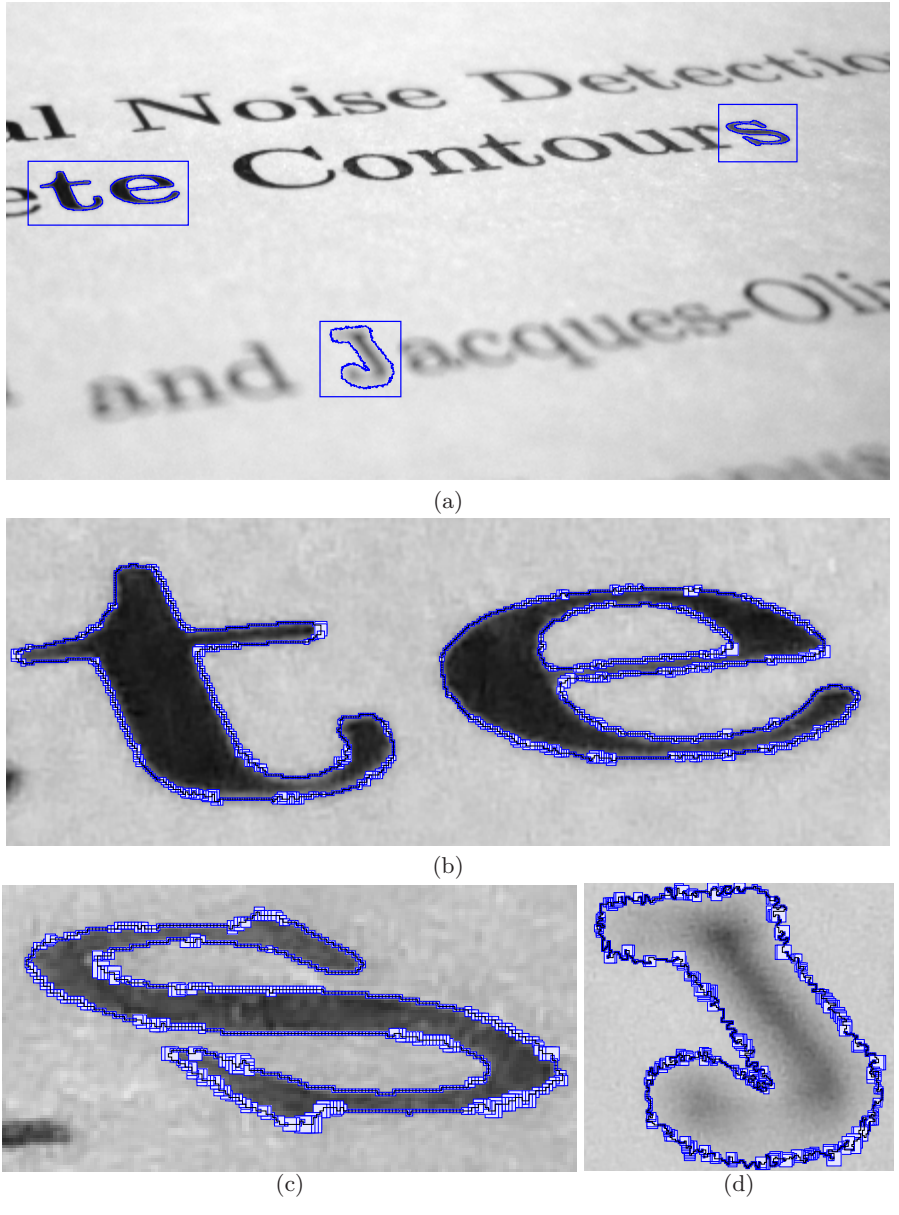

Fig. 8. Noise detection applied on a real text photography (a). The contours of the characters (b-d) were extracted by a simple threshold.

Timing Measures. To conclude the experimentation part some runtime measures were performed on the contours of Fig. 8. The times given on the following tabular were obtained on a 2.4 *GHz Intel Core Duo*. The measures include the computation of all subsampled contours $\phi_i^{x_0,y_0}(C)$ and their maximal segments.

nb points	226	702	788	874	1450
times (ms)	178	363	387	411	513

4 Concluding Remarks and Perspectives

In this paper we have proposed an original way to evaluate locally the noise level of a digital contour along with its meaningful scales. No parameter has to be tuned except the parameter associated to the maximal detectable noise level. Our experimentations confirm the efficiency of our approach, its independence to shape resolution and noise localisation. We thus expect that this approach will be used by many applications which are dependent on a noise or scale parameter. In future works, we plan to combine this approach with blurred segments to obtain unsupervised geometric estimators, precise on perfect zones and robust elsewhere.

References

1. Chen, K.: Adaptive smoothing via contextual and local discontinuities. IEEE Trans. Pattern Anal. Mach. Intell. 27(10), 1552–1566 (2005)
2. Debled-Rennesson, I., Feschet, F., Rouyer-Degli, J.: Optimal blurred segments decomposition of noisy shapes in linear times. Comp. and Graphics 30, 30–36 (2006)
3. de Vieilleville, F., Lachaud, J.O., Feschet, F.: Maximal digital straight segments and convergence of discrete geometric estimators. J. Math. Imaging Vis. 27(2), 471–502 (2007)
4. Elder, J.H., Zucker, S.W.: Local scale control for edge detection and blur estimation. IEEE Trans. Pattern Anal. Mach. Intell. 20(7), 669–716 (1998)
5. Kerautret, B., Lachaud, J.O.: Curvature estimation along noisy digital contours by approximate global optimization. Pattern Recognition 42(10), 2265–2278 (2009)
6. Koenderink, J.J.: The structure of images. Biol. Cyb. 50, 363–370 (1984)
7. Lachaud, J.O.: Espaces non-euclidiens et analyse d'image : modèles déformables riemanniens et discrets, topologie et géométrie discrète. Habilitation à diriger des recherches, Université Bordeaux 1, Talence, France (2006) (en français)
8. Lachaud, J.O., Vialard, A., de Vieilleville, F.: Fast, accurate and convergent tangent estimation on digital contours. Image Vision Comp. 25(10), 1572–1587 (2007)
9. Malgouyres, R., Brunet, F., Fourey, S.: Binomial convolutions and derivatives estimations from noisy discretizations. In: Coeurjolly, D., Sivignon, I., Tougne, L., Dupont, F. (eds.) DGCI 2008. LNCS, vol. 4992, pp. 370–379. Springer, Heidelberg (2008)
10. Nguyen, T., Debled-Rennesson, I.: Curvature estimation in noisy curves. In: Kropatsch, W.G., Kampel, M., Hanbury, A. (eds.) CAIP 2007. LNCS, vol. 4673, pp. 474–481. Springer, Heidelberg (2007)
11. Witkin, A.P.: Scale-space filtering. In: Proc. 8th Int. Joint Conf. Artificial Intelligence, pp. 1019–1022 (1983)